JOURNAL OF MATERIALS SCIENCE: MATERIALS IN MEDICINE 11 (2000) 235–246

# Three dimensional measurement of the surface topography of ceramic and metallic orthopaedic joint prostheses

L. BLUNT, X. Q. JIANG
*Center for Ultra Precision Engineering, School of Engineering, University of Huddersfield, Queensgate, Huddersfield HD1 3DH, UK*

The comprehensive study of surface topography of the orthopaedic joint prostheses has become very important for analysis of the wear mechanism and the performance life of the joint replacement systems. The aim of the study to investigate ''best'' methods for the three-dimensional (3D) surface metrology of orthopaedic joint prostheses. Characterization techniques for the identification and evaluation of the functional features of the bearing surface topographies has been provided in previous work [1]. This paper concentrates on addressing issues of measurement and application techniques for assessment of the 3D surface topography of the joint replacement systems by using contacting stylus instruments, atomic force microscopes (AFM), and non-contacting measurement supported by focus detection instruments and phase-shifting interferometers. The techniques are discussed according to different analysis requirements of the orthopaedic joint prostheses. This work also discusses the performances of the instruments in terms of the measurement of femoral heads. Finally, recommendations for acceptable measurement techniques and application for analyzing surface topography of orthopaedic joint prostheses are summarized.


## 1. Introduction

Surface topographies of the orthopaedic joint prostheses have attracted a considerable amount of research interest. Current statistical figures show that in the UK alone some 50 000 orthopaedic joint prostheses are implanted annually, while in the USA, the estimated number is up to approximately 200 000 [2, 3]. The surface topography of the counterface, the femoral head rubbing against the UHMWPE acetabular cup, has been recognized as one of the most important factors affecting the functional performance of the joint replacement system. A series of researchers have indicated that wear rate of the polymer acetabular cup is determined primarily by the surface topographical characteristics of the femoral head [3–21]. Hall, McGovern and Backnick [5–7] have shown that statistical roughness parameters of the retrieved femoral heads (37 explanted) are significantly greater when compared with values from newly prepared prostheses. Bauer [8] has found that if the initial surface roughness of new femoral heads is smoother than the standard manufacturing specifications, the retrieved cobalt-chrome heads have a lower surface roughness and less deep scratches than the those of heads with standard roughness values used in his clinical researches. Fisher and others [10–17, 19–21] have shown that the wear of the UHMWPE was greatly affected by the high counterface roughness. It was pointed out that it is essential to control the topography of the counterface of the femoral head to ensure the low wear rate in service. Also it has been reported that an increase in the surface roughness of the femoral head, $R_a$, from 0.0 1μm to 0.1 μm will cause a 13 fold increase in wear rate of the UHMWPE [18]. The wear of UHMWPE in artificial joints has been referred to as a critical determinant of the long term clinical performance of joint replacements. The wear particles and debris generated are liberated into the surrounding tissues of the joint causing adverse cellular reactions that consequently lead to bone resorption and loosening of the joint [8–20]. There is an important indication that there is a need to reduce the volume and numbers of UHMWPE wear particles in order to improve long-term clinical performance of total artificial joints.

The current standards [22, 23] for the measurement of the orthopaedic joint prostheses assume that traditional stylus instruments and two-dimensional (2D) profile techniques are used. In this case the surface roughness obtained in terms of these standards only addresses a part of the 3D surface topographical information of the bearing surface, while the other functional features of the bearing surface such as peaks, pits and scratches, cannot be clearly identified and separated. The measurement and analysis of the 2D profile or sections, even if properly controlled, can only give an incomplete description of the real surface topography. On the other hand, current clinical and simulated research has shown clearly that the

heads must be manufactured as smooth as possible in the belief that a smoother head can cause less wear of the acetabular cup. As a result, the manufacturers routinely produce heads with the mean value of profile, $R_a$, of $5 \sim 15$ nm whilst for alumina and zirconia heads $R_a$ is $< 5$ nm, which way below the levels of roughness assumed in these standards. This means that the traditional stylus instruments are at or even beyond their limit of resolution of surface deviations, for example 10 nm is quoted as the best vertical resolution currently possible using the commercially available stylus techniques. The measurement accuracy decreases further due to the quantisation errors, the errors in the mechanical datum of the instruments as well as the mechanical linkages. The lateral measurement accuracy is also limited by the finite stylus diameter (usually 2 or 5 μm) and the positional contact accuracy. Clearly, with the roughness of the heads at extremely low levels these errors play a significant part in the measured values.

It is very important that an adequate measurement knowledge is achieved if improvement in the joint performance is required. Overall the present work is an attempt to investigate the metrology techniques that should be implemented to more fully measure, characterize and interpret the surface topography of joint replacement systems. In this work, the measurement methods and corresponding instruments are outlined, and the 3D application and visualization techniques are presented. Recommendations of the acceptable measurement methods and techniques, for recovering the nature of the surface topography of orthopaedic joint prostheses, are provided.

## 2. The 3D surface measurement

The emergence of the 3D approach to surface analysis is largely due to the limitations of 2D surface analysis and also as a result of the development of modern powerful microcomputers. Recently, many 3D systems have been proposed and developed [26–44, 57, 59–63, 71–74], together with many 3D surface topography measurement techniques. Moreover, the European Community has supported a program of development of methods for 3D surface measurement and characterization [45]. Comprehensive research based on this European program was initiated with the aim of the development of a new fundamental, international 3D surface measurement standard [24, 25]. The functional performance of the surfaces can now be further quantified in terms of roughness using 3D surface measurement allied with conventional tribological and microscopy techniques. This is leading to a better understanding of the performance of functional surfaces. Furthermore, 3D surface measurement is already proving to be an invaluable tool in several aspects of advanced manufacturing engineering, tribology and material science etc. [25, 46–48]. The introduction of 3D surface measurement techniques into the field of the joint replacement systems has meant that the areas of application of topography analysis have undergone further expansion. The key to the expansion is that the measurements can be carried out using non-contacting instruments. These instruments reduce the levels of surface contamination, eliminate the possibility of surface contact damage and importantly allow relatively soft materials to be measured with a high accuracy. In the present study, the surface measuring techniques range from contacting stylus, optical focus detection instruments, optical interferometers to AFM's. This is in order to investigate techniques capable of measuring the surface topography with sufficient spatial and vertical resolution so as to fully address the surface topography of the orthopaedic joint prostheses.

### 2.1. Measurement methods

The 3D measurement methods can be classified based on different physical principles; stylus, optical and scanning microscopy as shown in Fig. 1. The stylus instruments are typically contacting methods, and optical instruments are non-contacting techniques, and scanning microscopy covers both contacting and non-contacting techniques.

#### *2.1.1. Stylus method*

The stylus method refers to instruments that use a mechanical probe via a transducer, such as an inductance transformer or an optical interferometer, to measure the displacement of the stylus as it moves across the surface. The principle schemes of the three transducers are shown in Fig. 2. The Fig. 2(a) illustrates a linearly variable differential transformer [49]. In this configuration, two coils are attached to the iron core fixed to one end of pick-up arm beyond the pivotal mounting. When stylus scans the measured surface, the iron core moves linearly within the coils, leading to a differential change in inductance. The altered electrical signal is amplified, processed and converted into a digital signal via an A/D converter then analyzed using a computer. The advantage of the traditional sensing system is that it has a simple structure and a good stability. The difficulty for this transformer is that it can not attain a high precision over a large measuring range. For this reason, a transducer based on interferometry has been developed [50–53]. As seen in Fig. 2(*b*), a Michelson interferometer is employed instead of the inductance transformer. At one end of the pick-up arm there is a reflector that acts as the measurement arm of the interference transducer. The interferometer has two equal optical paths. When the surface height varies, the length of optical path of the measurement arm will change, thus generating a fringe pattern of interference. The optical fringe signal is detected by photo detectors then fed into a preamplifier board producing the conventional quadrate signal that enables bi-directional counting and interpolation to the resolution of λ/128. The standard value of this transducer system depends on the wavelength of He-Ne laser. It has an extended dynamic measuring range, which makes it possible to measure with a large measuring range (6 mm) having a high resolution (10 nm). Some problems however may arise. Firstly, since the interference fringe pattern is determined by the optical path difference (OPD) of the Michelson interferometer, the stability of optical system which may vary with regard to the changes of atmospheric pressure and temperature, leads to incorrect measurement. Secondly, it has the disadvan-

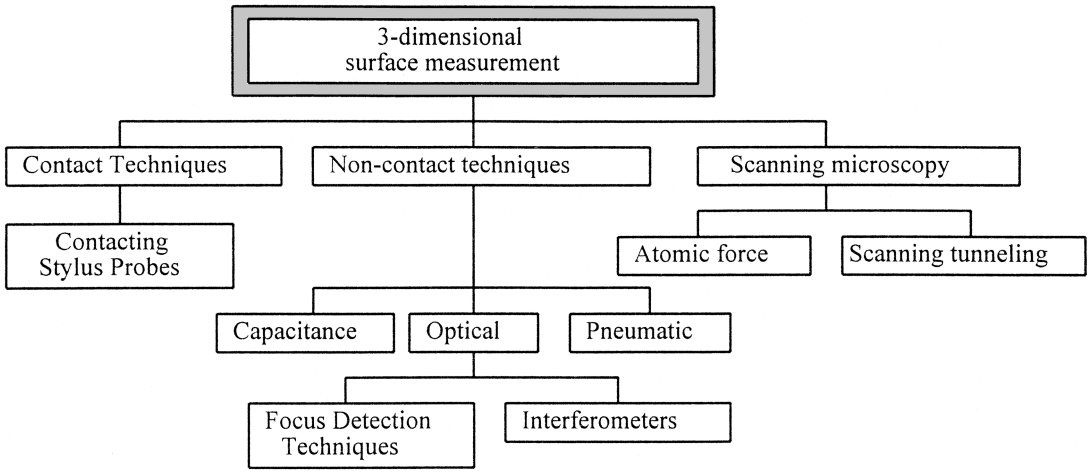


*Figure 1* Classification of surface topography instruments based on the physical principles of measurement.

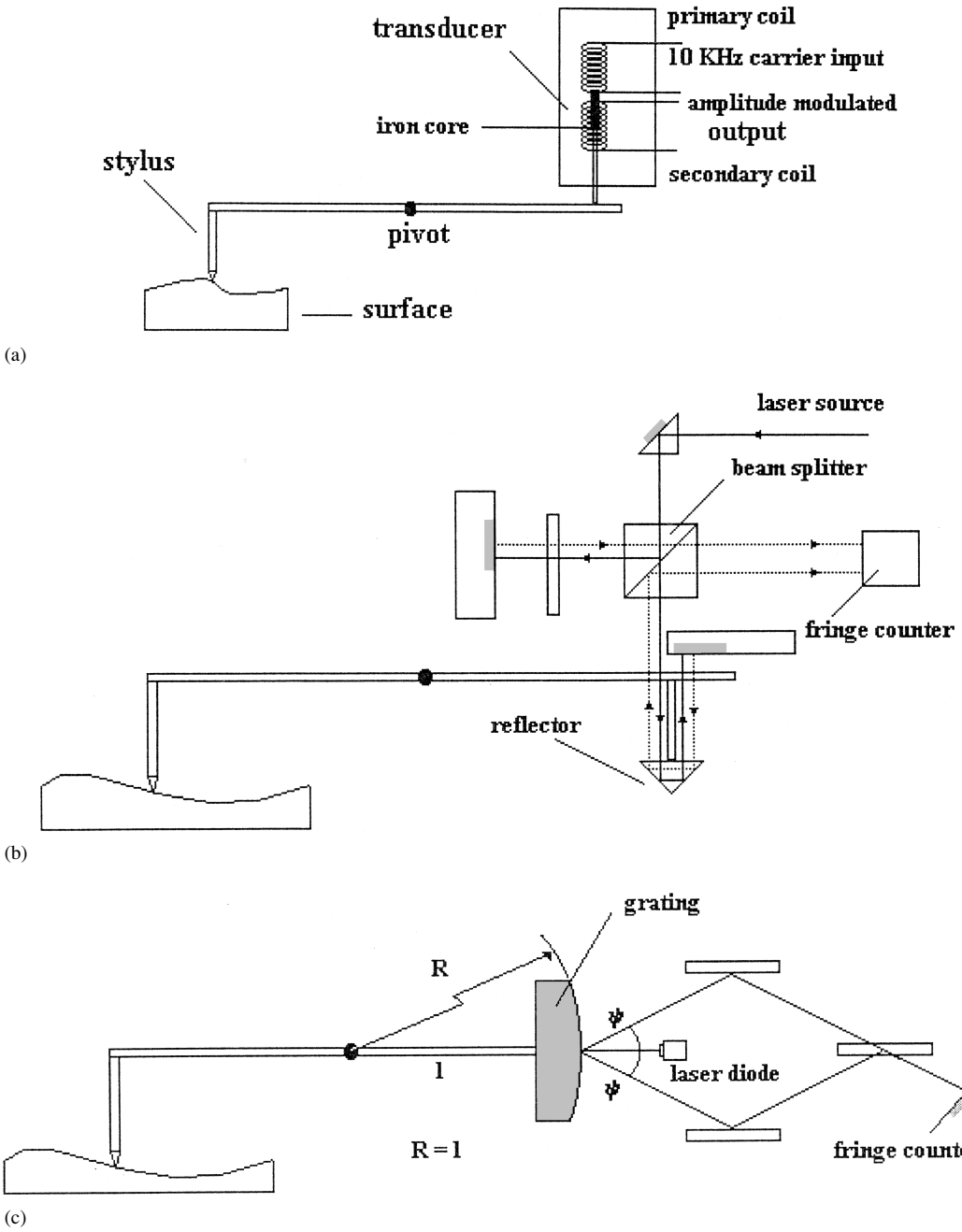


*Figure 2* The principle schemes of three transducers. (a) a linearly variable differential transformer, (b) a interferometric transducer based on a Michelson interferometer, (c) a grating transducer based on Doppler principle of the laser.

tage of a long optical path, complicated sensor structure and very expensive stable laser system. As a result, another newer transducer based on the Doppler principle of the laser has been developed as illustrated in Fig. 2(c) [54–57]. In the structure of the transducer, the grating constant of a Reflecting Cylindrical Hologram Diffraction (RCHD) grating acts as the standard reference. The stylus displacement will be measured precisely by detecting the beat-frequency fringe signal of phase changes of the RCHD grating. The grating interferometer is illuminated by employing a relatively cheap and low power semiconductor laser. The width of the fringe pattern produced by the grating interference equals half of the grating constant. The precision of grating interference transducer depends on the overlapping interference average effect of the diffracting wave over the many grating pitches, so that it has a strong property, having a high ratio of signal to noise and great resistance to disturbance. Similarly, the fringe signal is fed to specially designed hardware for back-forward fringe counting, and the A/D conversion is used to ensure the fine division of the RCHD grating signal with a nanometer precision [57]. The advantage of the RCHD grating transducer is that it not only gives a range to resolution ratio larger than $1 \times 10^6$, but also provides a compact configuration, a low cost, and a greater reliability.

Stylus methods for 3D surface analysis have developed from the existing 2D stylus techniques [28, 59]. 3D stylus measurement is realized through rastor scanning of the specimen surface. This method takes a number of closely spaced parallel profile traces that are referred to a common origin, to give the third dimension. This usually entails the use of $x$–$y$ axis translation tables or the existing gearbox of the 2D system and a single translation table. The accuracy in $x$–$y$ directions plays a fundamental role on the overall accuracy of the measurement. A uniform sampling strategy has been employed for 3D stylus measurement [24]. In this strategy, the size of sampling matrix is recommended to $M \times N$, $M = 2^p$, $p \leq 7$, $N = 2^q$, $q \leq 3$ in order to analyze the topography data by using various signal processing techniques. The sampling interval depends on the short wavelength limitation that includes the size of stylus tip and the horizontal resolution of the $x$–$y$ displacements. The main criteria in determining the sampling interval is to ensure that the significant components within the scale of interest can be measured without excessive distortion. Existing stylus systems can employ two kinds of data collection regimes; static or dynamic data collection [24]. For static collection, the stylus or specimen is moved to a defined position in the scanning routine where it stops and the height data at that point is measured, although the method is reliable it is excessively time consuming. In order to overcome this weakness the dynamic collection can be adopted, i.e. the height data is collected during the movement of the stylus. Dynamic data collection reduces measurement time however the system is limited by the dynamic characteristics of the stylus and high surface scanning speeds might lead to stylus ''bounce''. An important feature of 3D rastor scanning measurement is that the start points of all the scan traces should be in the same $y$–$z$ plane. This is accomplished through the use of precision lead screws, internal timing and velocity measurement or position transducers [60]. The nature of stylus measurement has proved to be its major drawback in that the loaded stylus can damage or scratch the surface. In addition, a further problem associated with stylus instruments for measurement of the orthopaedic joint prostheses is that the physical size of the stylus prevents it from penetrating small sharp surface pits and convolution effects can occur where sharp steps on a specimen surface tend to be smoothed.

### 2.1.2. Optical methods

*1. Focus detection instruments.* The focus detection instruments measure the height variation by maintaining the focus point of the optical system on measured surface. The measurement is carried via rastor scanning, as with mechanical stylus instruments. A schematic of a dynamic focus detection system is shown in Fig. 3(a). In the autofocusing system, a laser beam is focused onto the surface of the workpiece to be measured through a microscope objective. The projected light is reflected off the surface then collected by the same objective on a photo detector. This movement of the objective is controlled by a focal error signal obtained from an inductive transducer that diagnoses variations in the distance from its true focal point. When the focal point is on the surface, a photo detector gets the maximum intensity, and if the focal point is not on surface, the transducer sends out a focus error signal. The objective is moved precisely via a piezo-controller system according to focus error signal. The focal point is then returned to the surfaces. It is the movement of the piezo controlled objective which represents the surface height deviations. Generally, the metrology of the focus method depends on the high numerical aperture of microscope objective which directly affects the accuracy of the focus instruments [58]. For example, the vertical resolution defined by the size of the focal spot is inversely proportional to this numerical aperture; the maximum surface slope of the specimen detected is given by the numerical aperture. The sensitivity to the defocusing depends on increasing the numerical aperture. 3D measurement is realized by either fixing the laser sensor and rastor scanning the specimen beneath using *precision* $x$–$y$ tables. Alternately the scanning head can be translated in the $x$–$y$ plane while the specimen is held stationary. The original 3D measured data is transferred to a computer via an A/D converter where it is processed and the roughness parameters obtained. Other methods for focus detection reviewed by Stout [25] include differential detection, critical angle method, astigmatic method, Foucault method, skew beam method and the confocal method. Focus detection systems require a finite amount of light ( $> 5\%$) to be reflected back into the detector and consequently opaque surfaces cannot be measured. Additionally in case of steep slopes, the scanning focus spot invariably loses focus and rapidly searches for focus in the $z$ plane before ''finding'' the surface once again in the next scan position. This phenomenon can lead to spurious spikes and sharp pits being falsely registered in the surface data.

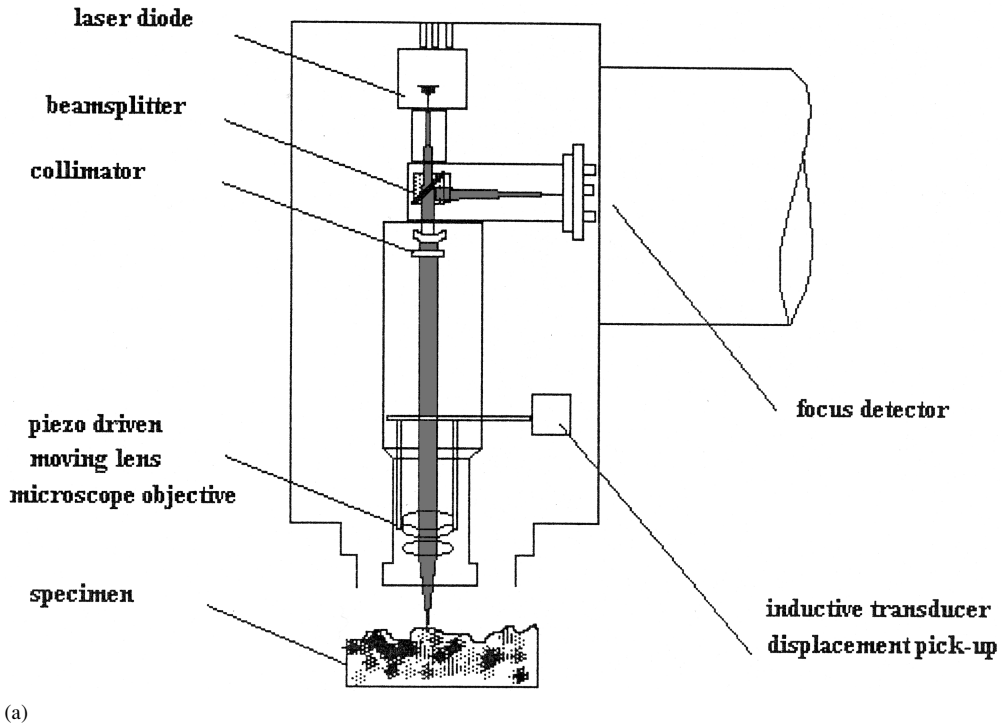


(a)

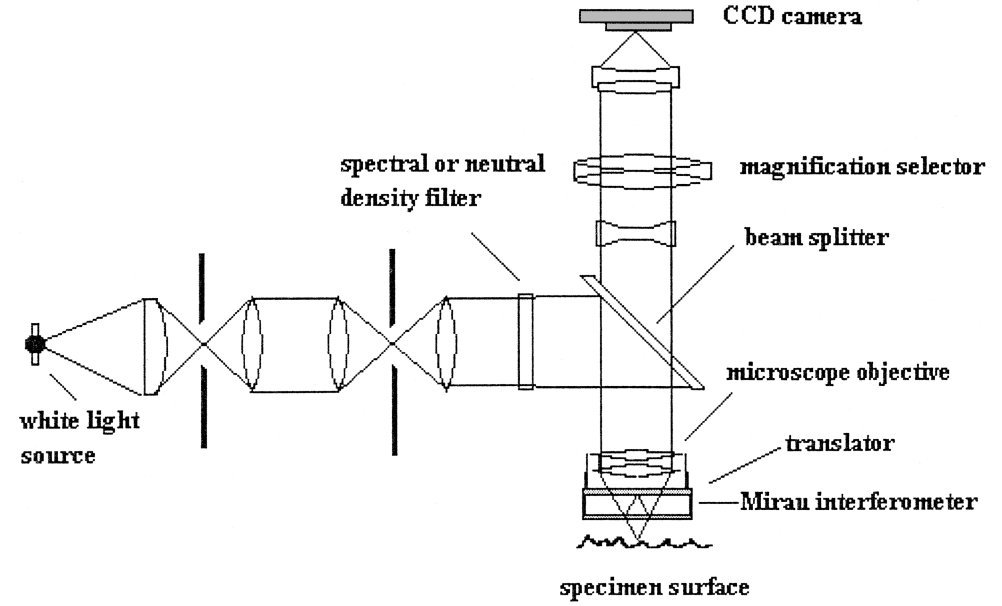


(b)

*Figure 3* Non-contacting measurement principles. (a) A schematic representation of a dynamic focus detection measurement system; (b) A schematic representation of a phase-shifting interferometer.

2. *Optical interferometers.* When measuring surfaces in the nanometer range, optical interference techniques can be employed. These systems work on the principle of interference of two beams of light where at least one is reflected off the surface of the specimen. The two most widely used techniques are phase-shifting interferometry and scanning differential interferometry [63–65]. Phase-shifting interferometry was first developed by Bruning [66] in 1974. This conventional phase-shifting interferometer based on He-Ne laser has a major drawback that discontinuous height variations of surface topography can result in interferometric phase ambiguities that are difficult or impossible to interpret. For this reason, new forms of innovative surface phase-shifting instruments have been proposed that are specially designed to function with white-light [67–69]. A schematic diagram of a phase-shifting interferometer based on white-light is shown in Fig. 3(b). An incandescent lamp illuminates an interferometric Mirau-type objective via a beam-splitter prism. The microscope objective shown in the Fig. 3(b) also has a beam-splitting element that transmits one portion of the beam to a reference mirror and the other beam to the specimen surface. The two beams reflected from the measured surface and the reference respectively are recombined and projected onto a charge-coupled device (CCD) video camera, which generates a signal proportional to the resultant beam intensity produced by the interference effect. The objective lens is translated by a piezo-electric fixture that is capable of precise vertical

scans. This has the effect of varying the optical path difference (OPD) of the interferometer. A sequence of intensity data frames is acquired by the camera and stored in microcomputer memory during a continuous vertical scan of the objective lens. Since good white-light fringe patterns appear only over a small portion of the scan, most of the raw intensity data can be discarded. For this reason, the acquisition speed and required processing of intensity data frames is very rapid. There are two methods to identify of the height of the measured surface. One technique is to detect the phase of a number of interference patterns produced by the two interfering wavefronts from the reference surface and the specimen surface. The phase is achieved by measuring three or more interference patterns each associated with a different axial position of the reference or specimen surface. The another method is that a white-light interferogram is considered to be a sum of a number of independent fringe patterns of various colors by incoherent superposition. Fourier analysis of the interferogram can recover these virtual single-color fringe patterns in order to determine their relative strength and phase as a function of wave number. Here, white light is not only a source of highly-localized fringes, but also a rich repository of multiple wavelengths that identify surface features with extraordinary accuracy [69–70]. The main drawbacks of interferometric measurement is the limitation to surfaces with a reasonable reflectivity ( $>$ 15%). The maximum vertical range of these systems is also limited to a level approaching the wavelength of the incident light and slope changes are sometimes difficult to measure with interferometric systems. New systems have recently become commercially available that have ranges as high as 600 μm being based on a variation of the phase shifting principle. A phase-shifting interferometer has a fixed sampling interval dependent on the magnification of the microscope objective and the size of the pixel of a CCD areal array. Thus the size of 3D image is fixed by those of the microscope objective and the CCD areal array. Finally a critical feature of interferometric measurement is that a high degree of environmental vibration isolation is required when operating the instrument if useful data is to be realized. This can cause problems in location of instrumentation in manufacturing environments.

### 2.1.3. Scanning probe microscopes and atomic force microscopes

Ultimate vertical resolution at the sub nanometer and angstrom level is attained through the use of scanning tunneling microscopes (STM) and atomic force microscopes (AFM). The scanning tunneling microscope was pioneered by Binning [71] and is shown in Fig. 4(a). In principle a conducting probe tip of nominally one atom diameter is driven within nanometers of the specimen surface. A bias voltage of 2 mV–2 V is then applied across the gap and electrons then tunnel across the gap. The monitored current is of the order of pA–nA. This current increases exponentially as the gap is decreased and for a 1 Å gap change the tunneling current changes by an order of magnitude. This sensitivity allows vertical resolutions of 0.01 Å. The scanning mode is usually

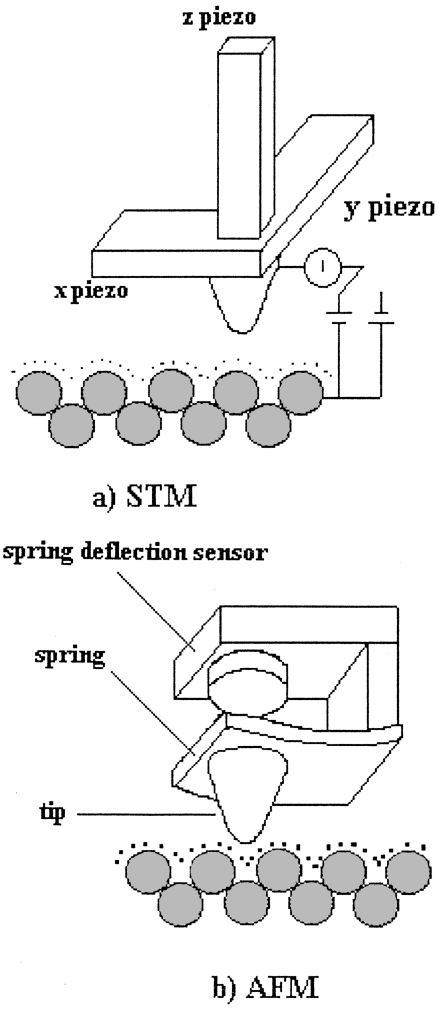


*Figure 4* Schematic representation. (a) A STM type surface measurement system; (b) An AFM surface measurement system.

based around a constant current feedback regime and rastor scanning. The $x$, $y$, and $z$ motions are realized by a tripod configuration of piezo-electric elements with recent instruments employing a piezo tube set-up for added speed and stability. This system allows lateral resolutions of 1 Å. A maximum of 5 μm is usually claimed for vertical range and a lateral range of $100 \times 100$μm [72–73]. One of the main limitations of the STM is that it is fact that only conducting materials can be measured. This proved to be one of the driving forces behind the development of the atomic force microscope by Binning and Quate [74]. In this case an ultra fine silica diamond tip is scanned across the specimen surface recording the inter atomic forces between the tip and the atoms of the sample, Fig. 4(b). The tip actually touches the sample and the mode of operation is much like that of a conventional stylus instrument. The tip force is tiny about $10^{-6} \sim 10^{-9} N$ and at such low forces the tip can trace over atoms without damaging the surface. The tip can be made from a fractured diamond fragment or silica and is attached to a cantilever system. The cantilevers are small and have high resonant frequencies, a typical cantilever of silicon oxide having a resonant frequency of 100 kHz. The deflection of the cantilever can be measured by means of an electron tunneling microscope (STM), an interferometer or by means of the deflection of a laser beam reflected off a mirror mounted on the back of the

cantilever. All of these require an electrical signal that varies rapidly with deflection. The signal is sent to the same electronics as used for the STM. A feedback circuit controls the voltage applied to the $z$ piezo element so that the signal is held constant as the tip is scanned across the surface. The vertical movement of the $z$ piezo element is directly related to the surface topography. The $x$, $y$ scanning mode is the same as that employed for the STM, i.e. piezo tripod or tube. Furthermore, some problems can arise from cantilever distortions and contamination when measuring with an AFM.

## 2.2. Range and resolution

Clearly, the above-mentioned instruments have specific vertical and horizontal measurement ranges for which they are best suited. Additionally certain of their physical attributes (such as probe size and geometry, transducer sensitivity, movement error, scan length, datum, scale resolution etc.) also define their window of performance. When comparing the performance of the different instruments however problems occur as to the criteria upon which comparisons should be made. Conveniently a method for delineating the effective working range has been developed by Steadman [75]. The method is based around the limiting response of the instrument to sinusoidal surface perturbations. The limiting factors considered are the vertical range and resolution, the horizontal range and resolution, horizontal datum and probe size/geometry. The analysis results in a working amplitude wavelength space (AW space) for the given instrument. An amplitude-wavelength plot for the above instruments is presented in Fig. 5. In the figure, the two axes represent the resolution (towards the origin of the axes) and the range (away from the origin of the axes) of the instruments both in vertical and horizontal directions. Each block in the figure indicates the working area of an instrument. The lengths of two orthogonal lines drawn from any point, $P$, in the area, gives an indication of the ratio of range to resolution, the longer the length, the bigger the ratio. The figure clearly shows that the specific working areas of the different instruments define the instrument's suitability for carrying out a given measurement. The large working area of the stylus instruments illustrates its wide applicability however its range does not extend into the areas where the roughness of femoral heads is expected to fall and thus it is clear that conventional stylus instruments are not ideally suited for this type of measurement. It should be noted that the STM/AFM systems have the highest resolution but limited range. Interferometric systems have high resolution but a greater range than the scanning microscopes.

# 3. Measuring and application techniques

In the present study, a number of alumina zirconia and metallic femoral joints have been measured utilizing stylus optical and scanning probe techniques. All of the instruments are fully calibrated under manufacturer's instructions. As far as possible, the identical areas were measured on the surface of the heads and acetabular cups. For the stylus instrument standard measurement conditions are indicated for 2D measurement, ISO 4288 1996 [76]. For 3D measurement the measurement areas chosen are $1 \times 1$ mm or $2 \times 2$ mm for the stylus and focus detection instruments, $242 \times 233\,\mu$m (maximum area size for an interferometer), for the optical interferometery techniques and approximately $30 \times 30\,\mu$m for the AFM.

## 3.1. Stylus measurements

Stylus instruments have been traditionally used for the measurement of the topography of the orthopaedic joint prostheses. Essentially they have been used as a quality monitoring and controlling tool for the manufacturing process of the head and acetabular cup products. Typical results of 2D measurement by using a Rank Taylor Hobson Form Talysurf stylus instrument, with a Mechilson interferometric transducer, are shown in Fig. 6. This particular instrument is situated in an environmentally controlled laboratory and is well maintained and regularly calibrated. The figure shows a trace taken across the polar of a polished acetabular cup, whilst a good representation of the surface is gained with $R_a$ of nanometer accuracy, it is unclear which of the valley type

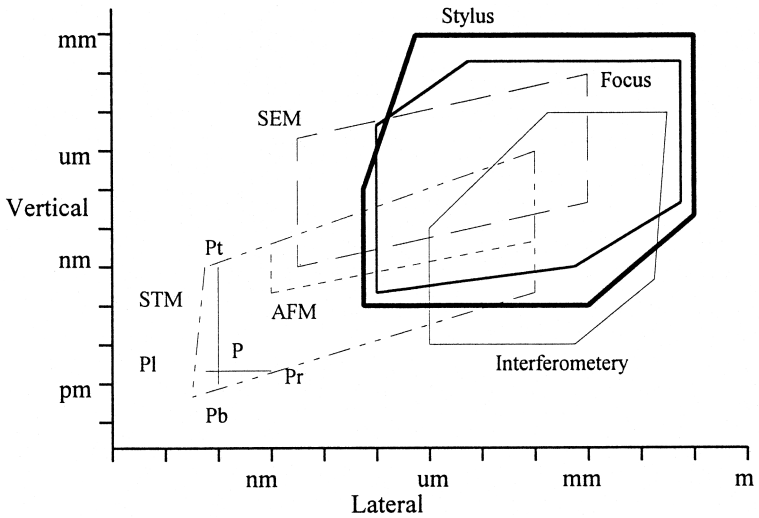


*Figure 5* An amplitude-wavelength plot for the above instruments.

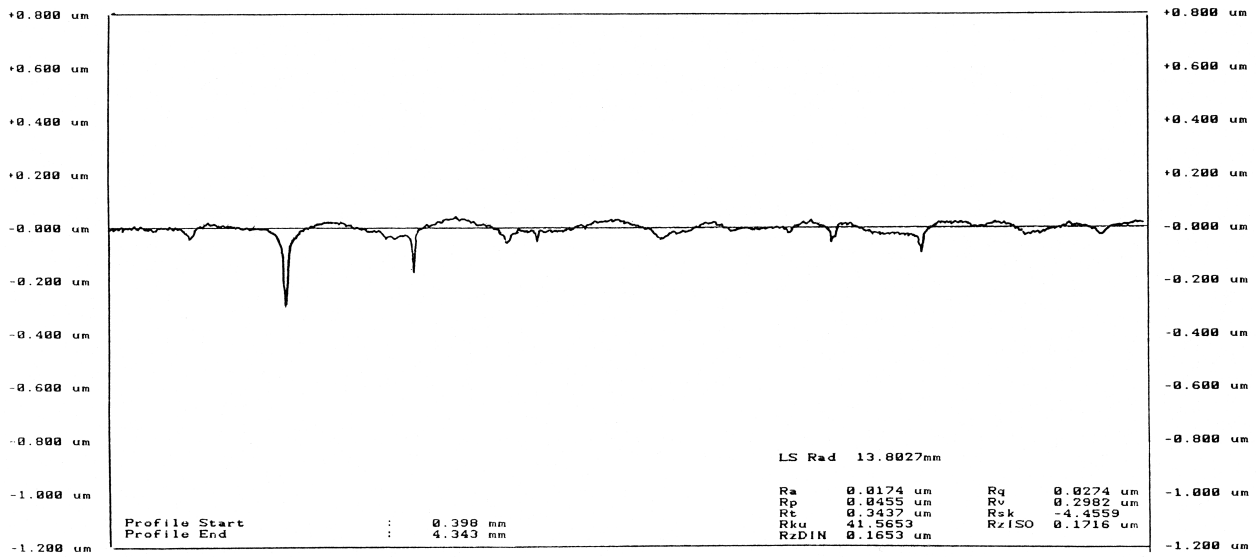


*Figure 6* 2D surface profiles of a polished acetabular cup taken across the polar region.

features indicate the presence of either pits or scratches. The presence of pits and scratches needs to be ascertained as they seriously affect the functional performance [22, 23]. Clearly to achieve this 3D surface measurement should be employed. To utilize commercial stylus techniques in a 3D sense a *x-y* translation tables and/or a gearbox is usually used for translation of the specimen. The tables are of a precision lead screw type shown as Fig. 7(a). Unfortunately, at the level of the topography deviations on polished surfaces, errors induced via the lead screw drive to the table become significant; and, in fact, clearly dominate as the results of a 3D gray scale map logged from the polar region of a ceramic acetabular cup indicate in Fig. 7(b). In this case the 3D drive is accomplished through the use of a single lead screw drive and the drive of the stylus gearbox hence the table error only affects one axes of measurement. The conclusion of these results is that unless dramatic improvements in the table drives used for scanning can be obtained the use of 3D stylus measurement should be avoided.

## 3.2. Focus detection techniques

Focus detection has been used for the measurement of femoral heads however these measurements may contain significant errors [77]. These appear as large spikes or pits in the data and occur as a result of optical phenomena. The presence of steps or pits and significant form deviation in a surface can also induce spikes in the data as the instrument ''hunts for focus'' or encounters interfering reflections causing ''rogue'' spikes and pits. This limits the use of the focus detection technique applied to the measurement of orthopaedic joint prostheses. As focus heads are translated in the same manner as stylus techniques, all of the table error problems associated with stylus measurement will also be present and contribute to measurement error. Fig. 8 shows an axonometric projection of 3D measurement of a metallic head and identifies the transient error and table errors when the spherical form is removed.

## 3.3. Phase-shifting Interferometer

The typical 3D imagines of the femoral head obtained by means of a WYKO TOPO 3D phase-shifting interferometer, with a sample interval of 1 μm and a $242 \times 233$μm sample Matrix, shown in Fig. 9. The bearing topographies of the two femoral heads ($Al_2O_3$ ceramic, and metallic) are obtained from different manufacturing processes. The Fig. 9(*a*) and Fig. 9(*c*) refer to the polar regions of the two heads respectively,

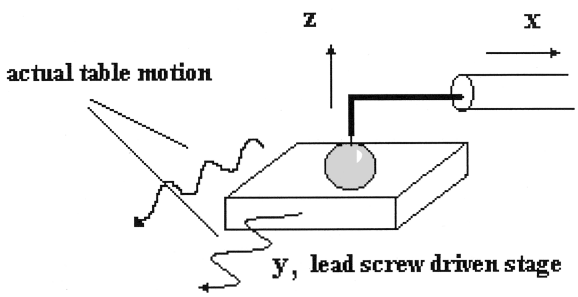


(a)

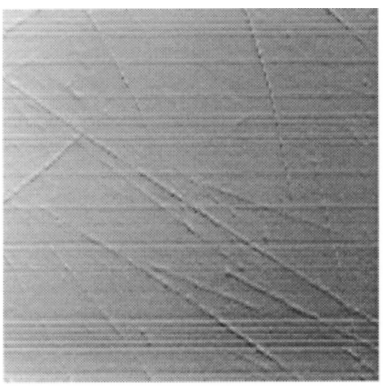

(b)

*Figure 7* The table scheme of a precision lead screw type. (a) Table movement; (b) A 3D surface map of a polished acetabular cup containing table error.

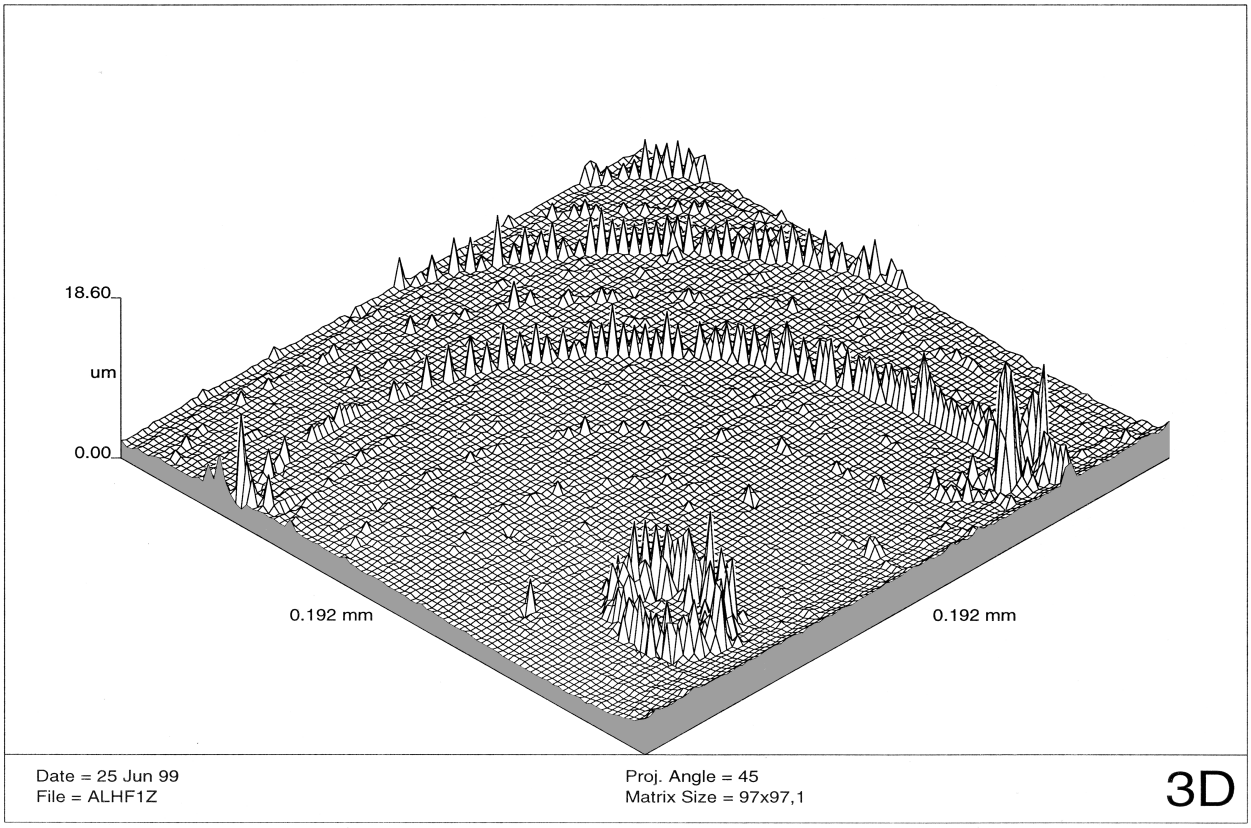


*Figure 8* Axonometric projection of 3D measurement of a metallic head measured using focus detection instrument.

whilst Fig. 9(*b*) and Fig. 9(*d*) refer to the equatorial regions of the heads. Analyzing these surfaces, the average surface roughness values were found to be similar $S_a = 4\,\text{nm}$ (ceramic) and $S_a = 10\,\text{nm}$ (metallic). Closer examination of the surface maps however revealed that the surfaces were quite different in nature. The ceramic head looks 'fine and smooth' except for a few isolated pits, peaks and some deeper scratches. The metallic surface displayed evidence of scratches from the polishing operation and also large ''drag'' pits resulting excessive polishing loads and/or times. Clearly interferometric techniques allow the surface topography to be viewed accurately and be fully recovered. In this case the topography produced as a result of the lapping operations gives a surface consisting of random scratches with occasional pits and peaks. The orientation extent and volume of which, will clearly impinge on the function of the joint.

### 3.4. Atomic force microscopy

For ultimate vertical and lateral resolution atomic force microscopy should be used. Fig. 10 shows a comparison of the surface topography of an alumina head with that of a metallic head. AFM allows the complex nature of the small scale topographical features produced by lapping/polishing to be viewed. In the figure the alumina head was measured in the polar region and shows a remarkably uniform lay with some cross hatching just evident. The metal head is also measured in the polar region and shows a random structure and also evidence of longer wavelength waviness running diagonally across the image. This is a much less controlled structure and in combination with the reduced hardness when compared to alumina heads could contribute to the increased wear rates when using metal heads. The roughness values were very close to those obtained by interferometric techniques.

### 3.5. Replication techniques

For the high accuracy acetabular cups direct measurement using an interferometer or an AFM is impossible. In this case, a replication technique can be used. The replication techniques should be treated with caution when dealing with nano level surface features. The relication involves the use of an acrylic solution which is poured over the surface region of interest and allowed to cure. However due to the fact that all liquid phases have finite viscosity and associated surface tension it is probably unlikely that the liquid phase fully penetrates the ultra fine machining scratches and pits on the surface. This would mean that the magnitude of these features will be underestimated. Despite this drawback it is possible to get highly accurate qualitative or semi-quantitative information at the ultra fine scales encountered on femoral heads, using the AFM, a clear indication of the nature topography can be obtained. The replicas can be measured in the conventional way however the data must be digitally inverted before characterization of the topography. Spherical form removal from the surface data is accomplished using digital filtering techniques.

## 4. Recommendations and conclusions

This paper has introduced 3D measurement techniques for surface metrology of the orthopaedic joint prostheses.

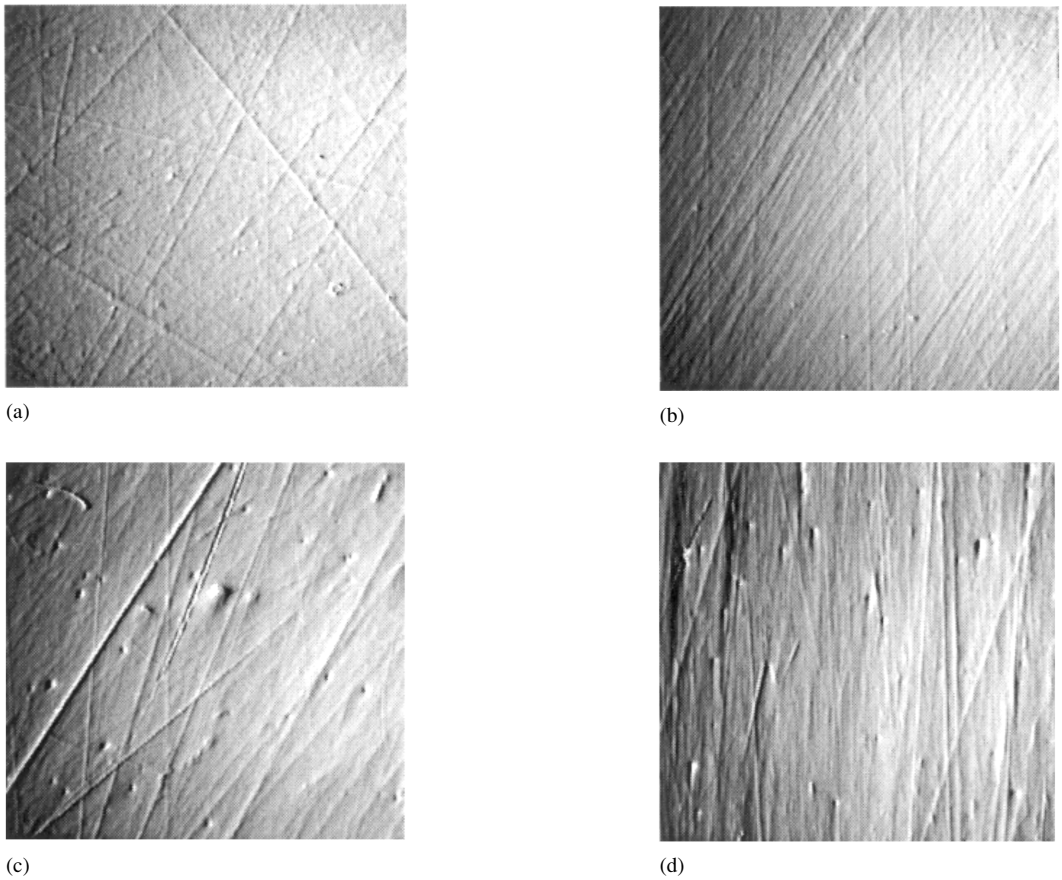


*Figure 9* Surface topographies of the two femoral heads measured using interferomentery. (a) The polar regions of the ceramic heads, (b) the equatorial regions of the ceramic heads; (c) the polar regions of the metallic heads; (d) the equatorial regions of the metallic heads.

As demonstrated above, 3D surface measurement can provide a tool for better understanding of the functional performance of bearing surfaces of the orthopaedic joint prostheses, although the measurement techniques are still developing with the modern mechanical, optical, electronic and computer technology advancing rapidly. Based on the above investigations, the following conclusions and recommendations are made:

1. In the 2D mode stylus instruments can be employed for monitoring and controlling the manufacturing process of the femoral heads though good environmental control and instrument maintenance is required. These instruments can be used for 3D measurement of the surface of the heads and acetabular cups only when the table errors can be corrected for by new digital techniques or improved translation devices.

2. The focus detection instruments can be used in manufacturing process of the femoral heads and acetabular cups when the slopes of scattering region on the bearing surface are less than standard critical angle limited by the objective numerical aperture.

3. The phase-shifting interferometers can offer the best method for 3D measurement of femoral heads due to large measurement range and nano-meter resolution.

4. AFM is ideal for description of the detail of surface

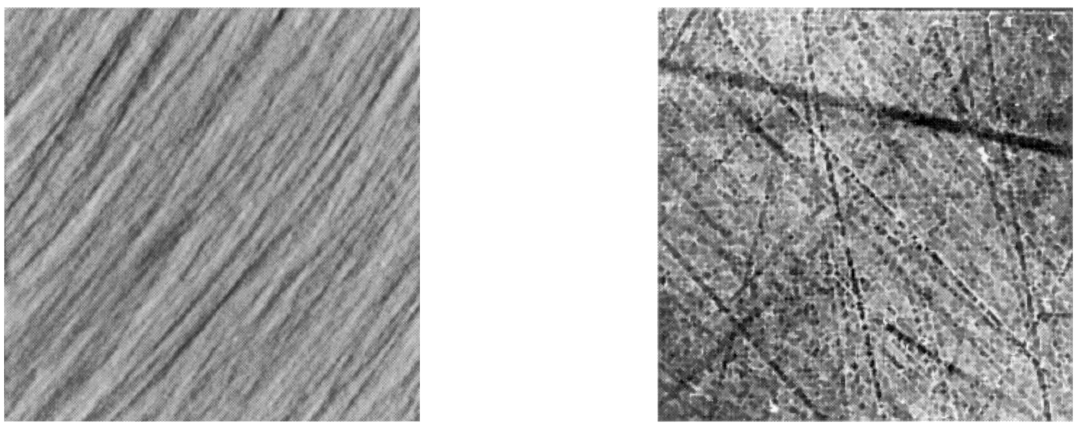


*Figure 10* AFM measurement of the polar region of the surface topography of (a) an alumna head and (b) a metallic head.

structure of the femoral heads though for full characterization many measurements need to be carried out.

The measurement and application techniques for the 3D surface topography of the joint replacement system have been introduced. The contacting and non-contacting measurement should be implemented according to different analyzing requirements of the orthopaedic joint prostheses. The potential applications of 3D surface topography of orthopaedic joint prostheses have been demonstrated. The recommendations of the acceptable measurement and application techniques for analyzing these surface topographies are summarized. Further work in this area will include characterization techniques for identification and evaluation of the functional features of these surface topographies have been provided [1]. For the feature identification, these surface topographies will be brought into a space-scale space, where these topographies can be investigated at variable scales with different resolutions. For the evaluation, the 3D surface assessment, techniques based on European program [24, 25], will be used for quantitative characterization of the various functional features of the orthopaedic joint prostheses. The authors' aim is to provide a complete tool for 3D Surface Metrology for orthopaedic joint prostheses.

## Acknowledgments

The authors would like to thank Dr Christina Doyle of Howmedica for her help and advice during this work.

## References

1. X. Q. JIANG, L. BLUNT and K. J. STOUT. *J. Inst. Mech. Eng. pt. H* **213** (1999) 49.
2. The *Daily Mail*, Nov. 17, 1995.
3. C. M. SHARKNESS, S. K. ACOSTA, R. M. MOORE, S. HAMBURGER and T. P. GROSS, *J. of Long-Term Effects of Medical Implants* **3** (1993) 237.
4. A. UNSWOTH, *Tribology International* **28** (1995) 485.
5. R. M. HALL, A. UNSWORTH, P. SINEY and B. M. WROBLEWSKI, *J. of Mater. Sci.; Mater. Med.* **7** (1996) 739.
6. T. E. MCGOVERN, J. BLACK, R. M. GRAHAM and M. LABERGE, *J. of Biomed. Mater. Res.* **32** (1996) 447.
7. M. BACHNICK, M. HASENPUSCH, H. RICHTER and U. BOENICK, *Biomedizinische Technique* **39** (1994) 302.
8. T. W. BAUER, S. K. TAYLOR, M. JIANG and S. V. MEDENDORP, *Clinical Orthopaedics and Related Research* **298** (1994) 11.
9. J. FISHER and D. DOWSON, *Proc. Inst. Mech. Eng.* **205** (1991).
10. J. FISHER, D. DOWSON, H. HAMDZAH and H. L. LEE, *Wear* **175** (1994) 219.
11. J. L. HAILEY, E. INGHAM, M. STONE, B. M. WROBLEWSKI and J. FISHER, *Proc., Inst. Mech. Eng.* **210** (1996) 3.
12. J. L. HAILEY, J. FISHER, D. DOWSON, S. A. SAMPATH, R. JOHNSON and M. ELLOY, *Med. Eng. Phys.* **16** (1994) 223.
13. J. R. COOPER, D. DOWSON, J. FISHER, G. H. ISAAC and B. M. WROBLEWSKI, *Clinical Materials* **14** (1993) 259.
14. H. ISHIKAWA, H. FUJIKI and K. YASUND, *J. of Biomechanical Engineering—Transactions of the ASME* **118** (1996) 377.
15. J. R. COOPER, D. DOWSON and J. FISHER, *Wear* **162** (1993) 378.
16. B. DERBYSHIRE, J. FISHER, D. DOWSON, C. HARDAKER and K. BRUMMITT, *Med. Eng. Phys.* **16** (1994) 229.
17. J. ZHAO and E. T. BROWN, *Quarterly Journal of Engineering Geology* **25** (1992) 279.
18. D. J. R. COOPER and J. FISHER, *Clin. Matls.* **14** (1993), 295.
19. J. FISHER and D. DOWSON, *Proc., Inst. Mech. Eng.* **205** (1991) 73.
20. J. FISHER, *Current Orthopaedics-Biomechanics Masterclass* **8** (1994) 164.
21. B. DERBYSHIRE, J. FISHER, D. DOWSON, C. HARDAKER and K. BRUMMITT, *Med. Eng. Phys.* **16** (1994) 229.
22. BS 7251, in ''Orthopaedic joint prostheses, Part 4'' (British Standard Organization, 1990).
23. ISO stand. 7206-2, in ''Implants for surgery—partial and total hip joint prostheses—Part 2'' (International Standard Organization, 1987).
24. K. J. STOUT, P. J. SULLIVAN, W. P. DONG, E. MAINSAH, N. LUO, T. MATHIA and H. ZAHYOUANI, in ''The development of methods for the characterization of roughness in three dimensions'' (Commission of the European Communities, 1993).
25. K. J. STOUT, in ''The three dimensions surface topography: measurement, interpretation and applications'' (Penton Press, London, 1994).
26. J. B. P. WILLIAMSON, *Proc., Inst. Mech. Eng.* **182** (1967–1968) 21.
27. J. PEKLENIK and M. KUBO, *Annals of the CIRP* **16** (1968) 257.
28. S. SAYLES and T. R. THOMAS, *J. of Physics E: Scientific Instruments* **9** (1976) 855.
29. T. TSUKADA and K. SASAJIMA, *Wear* **71** (1981) 1.
30. A. F. GEORGE and S. J. RADCLIFFE, *ibid.* **83** (1982) 327.
31. L. D. CHIFFRE and H. S. NIELSEN, *Precision Engineering* **9** (1987) 59.
32. T. KANADA, T. KUBSTA and A. SUZAKI, *Measurement Science and Technology* **2** (1991) 191.
33. T. V. VORBURGER, *Annals of the CIRP* **36** (1987).
34. The 3D digital surface topography and analysis system, Product Information (3D Digital Design and Development Ltd, 1991).
35. Surfascan 3D profilometer universal d'etats de surface bi et tridimensinnel. Product Information, (Somicronic, 1991).
36. B. SNAITH, M. J. EDOMONDS and S. D. PROBERT, *Precision Engineering* **3** (1987).
37. N. IDRUS, *Precision Engineering* **3** (1981).
38. E. C. TEAGUE, F. E. SCIRE, S. M. BAKERA and S. W. JENSEN, *Wear* **83** (1982) 31.
39. M. CHUARD, A. C. ROUDOT and J. MIGNOT, *ibid.* **96** (1984).
40. M. CHUARD, J. MIGNOT, P. NARDIN and D. RONDOT, *J. of Manufacturing System* **6** (1987).
41. J. T. HATAZAWA, K. YAMADA and T. HAWAGUCHI, *Surface Topography* **1** (1988).
42. S. J. RADCLIFFE and A. F. GEORGE, *Surface Topography* **1** (1988).
43. J. SULLIVAN, V. POROSHIN and C. HOOKE, *J. of Machine Tools and Manufacturing* **32** (1992).
44. H. DAGNALL, (RTH. Ltd. 2nd Ed., 1986).
45. C. Contract No 3374/1/0/170/90/2, University of Birmingham and L'Ecole Centrale de Lyon.
46. P. M. LONARDO, H. TRUMPOLD and L. CHIFFRE, *Annals of the CIRP* **45** (1996) 589.
47. I. SHERRINGTON and E. H. SMITH, *Wear* **125** (1988) 271.
48. I. SHERRINGTON and E. H. SMITH, *ibid.* **125** (1988) 289.
49. T. R. THOMAS, in ''Rough surface'' (Longman Inc, 1982).
50. Form and surface texture measurement (Rank Taylor Hobson, 1992).
51. J. D. GARRATT, *Precision Engineering* **4** (1982) 145.
52. J. D. GARRATT, W. J. BATES and M. J. PLAYER, UK Patent Application No. GB 2070276 A.
53. Prospectus for Form Talysurf (Rank Taylor Hobson Ltd, 1989).
54. I. K. BUEHRING and D. MANSFIELD, International Patent Application No. PCT/GB92/00975.
55. X. Q. JIANG, T. B. XIE, S. J. XIAO and L. ZHU, China Patent Application No. 94 1 01873.3.
56. X. Q. JIANG, T. B. XIE, C. X. YAO and L. ZHU, *SPIE* **2101** (1993) 554.
57. X. Q. JIANG, PhD Thesis, China, (1995).
58. HILLMAN, *Annals of the CIRP* **39** (1990) 581.
59. E. J. DAVIS, K. J. STOUT and P. J. SULLIVAN, *Industrial Metrology* **1** (1990) 193.
60. Y. FAINMAN, E. LENZ and V. SHAMIR, *Applied Optics* **21** (1982) 3200–3208.
61. HAMILTON and T. WILSON, *Applied Physics* **B** (1982) 211.

62. N. KOHNO, OZAWA, K. MIYAMOTO and T. MUSHA, *Applied Optics* **27** (1988) 103
63. W. P. DONG, K. J. STOUT, P. J. SULLIVAN, L. BLUNT and E. MAINSAH, to be published.
64. WYANT, C. L. KOLIOPOULOS, B. BHUSHAN and O. E. GEORGE, *ASLE Transactions* **27** (1984).
65. T. C. BRISTOW, *Surface Topography* **1** (1988) 85.
66. BRUNING, D. R. HERRIOTT, J. E. GALLAGHER, D. P. ROSENFELD, A. D. WHITE and D. J. BRANGACCIO, *Applied Optics* **23** (1974) 2693.
67. J. C. WYANT, *Laser Focus World* **131** (1993).
68. E. WOLF, *Elsevier Science* (1988) 357.
69. P. D. GROOT and L. DECK, *J. of Modern Optics* **42** (1995) 389.
70. P. D. GROOT and L. DECK, *Optical Letter* **18** (1993) 1462.
71. G. BINNING, H. ROHRER, C. GERBER and E. WEIBEL, *Applied Physics Letters* **40** (1981) 178.
72. ''The Scanning Probe Microscope Book'' (Burliegh Instruments Inc., 1991).
73. KUK and P. J. SILVERMAN, *Review of Instrument* **60** (1989) 165.
74. G. BINNING, C. F. QUATE and C. GERBER, *Physical Review Letters* **56** (1986) 930.
75. M. STEADMAN, *Precision Engineering* **9** (1987) 149.
76. ISO stand. 4288, in ''Surface texture: Profile method—Rules and procedures for the assessment of surface texture'' (International Standard Organization, 1996).
77. K. J. STOUT and L. BLUNT, *Surface Coatings and Technology* **71** (1995) 69.

*Received 30 July 1998*
*and accepted 21 June 1999*